J. Biomechanics, 1977, Vol. 10, pp. 325–337. Pergamon Press. Printed in Great Britain

COMPACT BONE FATIGUE DAMAGE—I. RESIDUAL STRENGTH AND STIFFNESS*†

D. R. CARTER and W. C. HAYES‡
Department of Orthopaedics, University of Washington, Seattle, WA 98195, U.S.A.

Abstract—Residual strength and stiffness of compact bovine bone specimens during fatigue were investigated and the fracture surfaces were examined by scanning electron microscopy. Residual strength tests consisted of rotating bending fatigue followed by tensile tests to failure. Specimens loaded to 50% of their fatigue lives had approximately a 13% loss of tensile strength ($p < 0.01$). Specimens tested in zero to tension axial fatigue showed a gradual loss of stiffness which in some specimens was greater than 20% at failure. These results indicate that repeated loading of bone causes a progressive loss of strength and stiffness. A similar fatigue behavior in composite materials is attributable to cumulative microcracking, debonding, void growth, and fiber breakage.

INTRODUCTION

The skeletal system protects vital organs from accidental injury, supports the body tissues, and facilitates movement. In fulfilling these tasks the bones are subjected to repeated stresses which may lead to microscopic damage (Radin *et al.*, 1973; Chamay, 1970; Nash, 1966). The normal healing response of biological tissues serves to repair this damage and maintain the structural integrity of the skeletal system (Nash, 1966; Frost, 1966). If damage accumulates faster than it can be repaired, pathological conditions may result. The process of fatigue damage accumulation has been implicated in fatigue (or stress) fractures (Devas, 1975; Morris and Blickenstaff, 1967), pathological fractures (Schneider and Kaye, 1975; Devas, 1965) and degenerative disorders (Radin *et al.*, 1973).

Fatigue is the progressive failure of a material under cyclic or fluctuating loads. This study examined the fatigue behavior of compact bone specimens *in vitro* and thus does not consider the *in vivo* healing response which may extend the fatigue life or prevent fatigue failure. While this approach may at first seem to have serious shortcomings, it does have many advantages. The interactions between mechanical damage and bone repair may be very complex. *In vitro* testing allows one to eliminate these interactions and isolate the process of mechanical damage. Once this process is fully understood, future studies of *in vivo* bone fatigue can proceed on a more rational basis.

A review of previous *in vitro* research on the stress-related fatigue properties of bone is provided by Evans (1973). More recently, Gray and Korbacher (1974) examined the compressive fatigue properties of compact bone. Carter (1976), Carter and Hayes (1976) and Carter, Hayes and Schurman (1976) determined quantitative relations for compact bone fatigue life as a function of stress amplitude, temperature, density and microstructure. Wright and Hayes (1976a) studied *in vitro* crack propagation in pre-cracked bovine bone specimens subjected to repeated loading. A crack growth-rate law relating crack growth to the stress intensity factor was derived. Previous investigations of compact bone fatigue behavior have been concerned primarily with determining the total fatigue life of bone under various conditions. Although tests of this type provide meaningful data on the total fatigue life of a material, they provide no information about the basic nature of fatigue damage. The accumulation of damage and possible changes in bone mechanical properties during the fatigue process have not been studied.

Before attempting to characterize the nature of fatigue damage in bone, it is reasonable to examine the fatigue behavior of other materials. Although metals and composite materials fail in fatigue, the fatigue process in metals is quite different from that of composites. In metals, repeated loading causes the accumulation of plastic strains and associated plastic slip lines which lead to fatigue crack initiation (Reed-Hill, 1964). Fatigue cracks propagate under repeated loading until final catastrophic failure occurs. Metals subjected to repeated loading do not exhibit a loss of stiffness or ultimate strength until after the crack is initiated (Salkind, 1972; Yang and Trapp, 1974). Composite materials fail in fatigue by widely distributed damage processes which may include delamination, matrix crazing, fiber failure, void growth and matrix cracking (Salkind, 1972). As a result, a composite material often exhibits a more gradual and progressive loss of stiffness and strength throughout its fatigue life (Salkind, 1972; Owen and Howe, 1972; Allen, 1971).

The fatigue behavior of a material is related to its behavior under a single applied loading to failure (Salkind, 1972). Compact bone specimens loaded to failure in tension were shown by Burstein *et al.* to exhibit a stress/strain curve consisting of an elastic

* *Received 6 December* 1976.
† This research was supported by the National Science Foundation through the Center for Materials Research at Stanford University.
‡ Department of Orthopaedic Surgery, University of Pennsylvania, Philadelphia, PA 19174, U.S.A.

region followed by yield, a flatter postyield regime, and failure (Currey, 1975; Burstein *et al.*, 1972, 1973). Metals and some composite materials exhibit similar loading curves. However, the micromechanical events at yield and postyield for metals are very different from those of composites. Yielding in metals is caused by plastic flow and is accompanied by the formation of plastic slip lines. A metal specimen loaded into its postyield regime, unloaded, and subsequently reloaded exhibits little or no loss of stiffness and no loss of ultimate strength. In composite materials the postyield regime is caused by multiple damage modes such as microcracking, debonding, void growth and fiber breakages. A composite material loaded into the postyield regime, unloaded, and subsequently reloaded typically exhibits a loss of stiffness and ultimate strength. Insights into the mechanical nature of yielding in a material may therefore be gained by studying its behavior under repetitive loading.

Recent investigations of the mechanical behavior of bone have led to controversy on the nature of yielding in bone. Chamay and Tschantz (1972) reported histological evidence of "plastic slip lines" in canine ulnas subjected to repeated loading both *in vivo* and *in vitro*. Burstein *et al.* (1973) and Reilly and Burstein (1974) demonstrated yielding in compact bone specimens and stated that this was evidence of plasticity. Burstein *et al.* (1975) hypothesized that yielding is caused by failure of the mineral phase of bone. They suggested that the postyield regime and secondary modulus observed in monotonic loading are due to the ability of unbroken collagen fibers to sustain load long after the failure of the less compliant mineral phase. Ascenzi and Bonucci (1976) demonstrated pronounced stress/strain nonlinearities in single osteons subjected to tensile loading. They attributed this behavior to progressive fracture of collagen fibers in adjacent lamellae.

In this study the residual strength of compact bone specimens subjected to repeated loads was examined. In addition, stress/strain curves of several specimens were monitored during tensile fatigue tests to obtain information about the changes in specimen stiffness during fatigue. The data of this study help to characterize the process of fatigue damage accumulation in bone. In addition, the results provide insights into the micromechanical nature of yielding in bone.

MATERIALS AND METHODS

Residual strength

Identical procedures were followed in the machining and storage of 115 bone specimens prior to testing. The mid-diaphysis of fresh beef femora were cut out with a band saw, each femur providing an annulus of cortical bone approx. 5.7 cm long. Longitudinal saw cuts through the annulus produced up to ten pieces of bone which were roughly 0.95 × 0.95 × 5.7 cm. These pieces were turned on a lathe to 0.635 cm dia. cylinders and the lengths reduced to 4.45 cm. A central waisted section was then made by rotating each dowel-shaped bone in the lathe and using a cutting tool mounted on a rotating pivot of the lathe toolpost (rotation radius = 1.27 cm). The tip radius of the tool was approx. 0.5 mm and the feed of the final finish was *ca.* 0.05 mm per revolution. The specimens were kept cool and wet by dripping water over them during all lathe work.

The final test specimens were therefore 4.45 cm long with a 0.635 cm dia. and contained a central waisted section of 0.475 cm dia. (Fig. 1). The specimen central axis was parallel to the longitudinal axis of the femur. Immediately after machining, the specimens were equilibrated in Ringer's solution overnight. They were then removed from solution and stored at −20°C (Wall *et al.*, 1970; Sedlin and Hirsch, 1966). After all of the specimens had been stored, they were randomly allocated to three test groups as follows: (1) tensile tests to failure—35 specimens; (2) fatigue tests to failure—30 specimens; (3) residual strength tests—50 specimens.

The tensile tests to failure were conducted with the specimens immersed in water at 37°C (Fig. 2). Testing was done on an electrohydraulic testing system (MTS, Minneapolis, Minnesota) at a constant piston stroke velocity of 0.01 mm/sec (corresponding to a strain rate of approx. 0.001 sec^{-1}). Load-displacement curves were recorded for all specimens using a Honeywell *X-Y* chart recorder. A linear variable differential transformer (LVDT) in the loading piston was used to measure displacements. In addition, the ultimate load was recorded for each specimen on an oscilloscope to provide a check on the chart recording system.

Fatigue tests were conducted with a Budd RBF-200 rotating beam fatigue testing machine. Testing procedures were identical to those described by Carter and Hayes (1976). However, all tests were done with a nominal stress amplitude of 86 MN/m^2 at a temperature of 37°C. Approximately 1.1 cm of the specimen on both ends was held by the machine collets. The stress amplitude in the waisted section was established by adjusting the bending moment applied to the specimen by the machine. The bone samples were rotated about their long axis at 125 cycles per sec and thereby subjected to a fully reversed, constant-amplitude cyclic loading with zero mean stress. Testing proceeded until complete failure occurred. A cycle

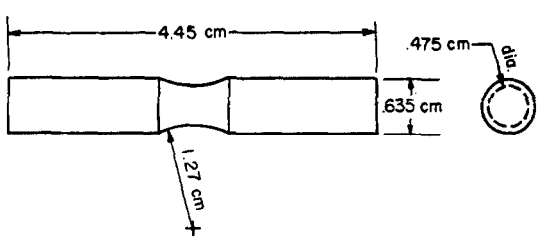

Fig. 1. Dimensions of residual strength specimens.

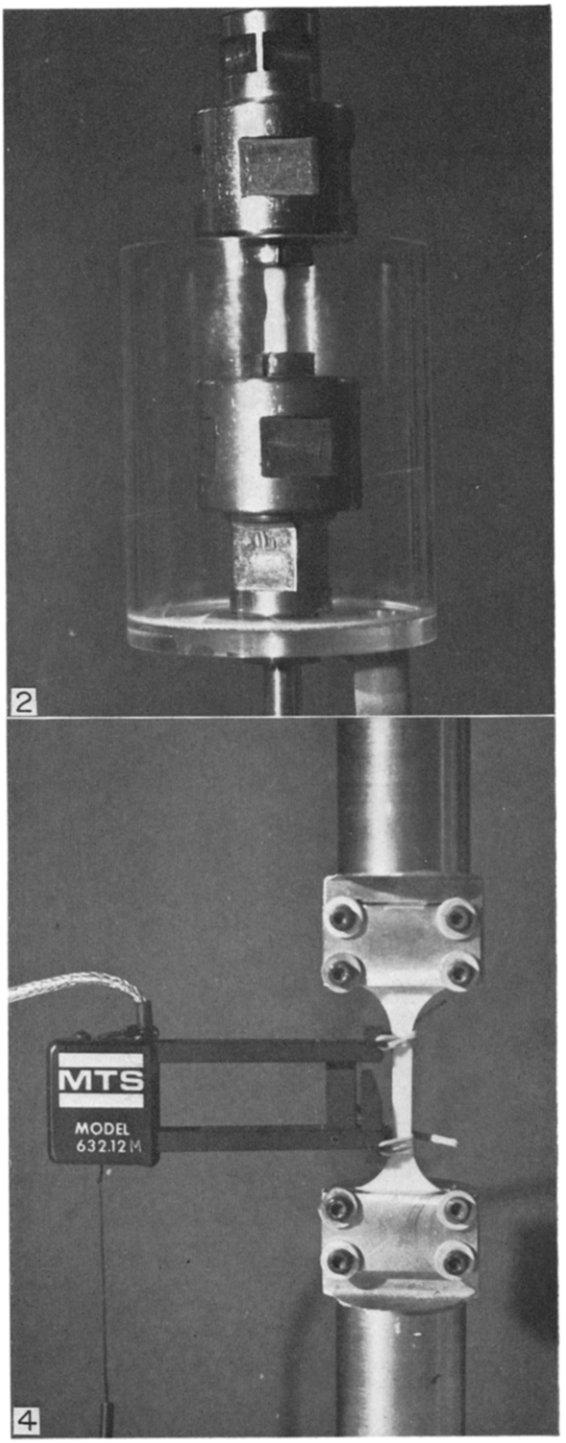

Fig. 2. Tensile strength test fixture.

Fig. 4. Residual stiffness test fixture with extensometer attached.

counter on the fatigue machine stopped when the specimens broke, thus automatically recording the number of cycles to failure.

The fifty residual strength specimens were fatigued in rotating bending for a varying number of cycles. The nominal load amplitude was 86 MN/m^2 and the test temperature was 37°C. The fatigue procedure was identical to that described for specimens tested to failure in fatigue. However, after a predetermined number of loading cycles, the unbroken specimens were removed from the fatigue machine. The specimens were then subjected to tensile tests to failure following the same procedures described earlier. The residual tensile strengths as well as the corresponding number of fatigue loading cycles were recorded.

A rough estimate of the microstructure of each specimen was made before mechanical testing. These estimates were based on the staining patterns which appeared when a specimen was dipped in a very dilute food-coloring solution. The characteristic staining patterns for secondary Haversian bone were distinctly different from those of primary bone. Estimates of specimen microstructure were especially helpful in the residual strength testing. Carter *et al.* (1976) showed that secondary Haversian specimens have a fatigue life approximately one-tenth of primary bone. Estimates of microstructure were therefore used as a guide in determining how long a specimen should be fatigued before residual tensile strengths could be determined.

It was anticipated that a great deal of data scatter would be encountered in this experiment due to variations in microstructure and density among the bone specimens. In addition, inhomogeneities in the structure of particular specimens might cause significant scatter. Residual strength tests were done in tension rather than bending in an effort to reduce the scatter caused by specimen inhomogeneities. In bending tests to failure, the ultimate strengths are greatly influenced by the orientation of the plane of bending with respect to specimen inhomogeneities. Tensile strengths, however, are unaffected by the orientation of the specimen in the grips.

To help account for data scatter among the test specimens, determinations of the microstructure and density of each specimen were made after testing. Cylindrical sections approx. 1 cm long were cut with a diamond saw from one end of each specimen away from the fracture site. These sections were thoroughly dried by placing them in an oven 70°C for five d. All of the samples were then weighed and their diameters and lengths determined with a micrometer. The dry density of each specimen tested was estimated on the basis of these measurements. Microstructure examination of the specimens was done by cutting away small cross sections of bone near the fracture site. These samples were ultrasonically degreased in trichloroethylene, embedded in plastic, polished, and photographed in a reflected light microscope.

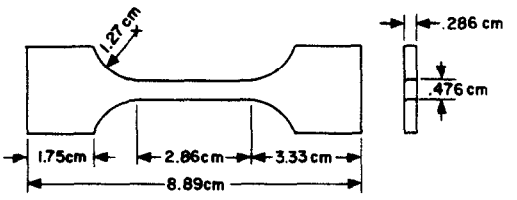

Fig. 3. Dimensions of residual stiffness specimens.

Residual stiffness

Eight longitudinally oriented specimens were machined from the diaphysis of fresh bovine femora and tibiae. The geometry of these specimens is shown in Fig. 3. The specimens had a central gage length of 25.4 mm with a rectangular cross section of 3.175 by 4.82 mm. The specimens were kept cool and wet by dripping water over them during all machining. Immediately after machining the specimens were equilibrated in Ringer's solution overnight. The following morning, they were removed from solution and stored at −20°C until testing (Sedlin and Hirsch, 1966).

Before testing, each specimen was equilibrated in water at room temperature (approx. 21°C). Water-soaked cheesecloth was wrapped around the gage length and an extensometer with a built-in strain gage bridge was attached. The specimen was then subjected to zero to tension fatigue tests at a loading frequency of 0.1 Hz on the MTS electrohydraulic testing system (Fig. 4). A haversine loading program was used and load/strain curves were continuously monitored on an oscilloscope. In addition, the Honeywell chart recorder was used to record selected loading and unloading curves at various times during the tests.

RESULTS AND ANALYSIS

Residual strength

Typical stress/displacement curves for the tensile tests to failure are shown in Fig. 5. Primary bone

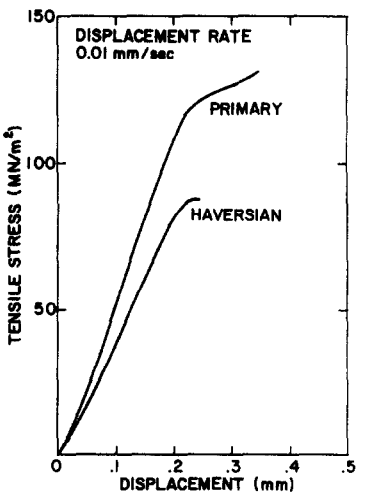

Fig. 5. Typical stress/displacement curves for tensile tests to failure.

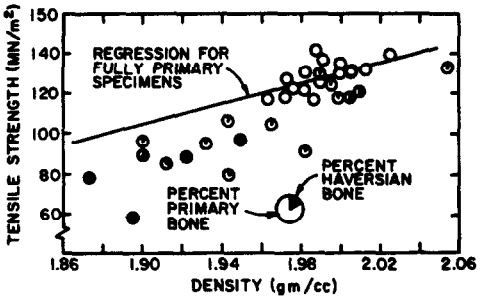

Fig. 6. Tensile strength vs density for specimens with no prior fatigue loading.

specimens generally exhibited greater stiffness, yield strength, and ultimate tensile strength than secondary Haversian specimens. The relationships between ultimate tensile strength, microstructure and density are shown in Fig. 6. The ultimate tensile strength of the primary bone specimens was 127.8 MN/m^2 (S.D. = 7.8, No. of specimens = 17). The ultimate strength of the four specimens with a fully secondary Haversian microstructure was 80.3 MN/m^2 (S.D. = 16.8).

A linear regression analysis of only the primary specimens revealed a weak but significant correlation between ultimate strength and density ($r^2 = 0.427$, $P > 0.01$). The relationship between predicted bone tensile strength ($\bar{\sigma}_0$, MN/m^2) and bone density (ρ, g/cm^3) was expressed as:

$$\bar{\sigma}_0 = A\rho + B \text{ (Primary bone)} \qquad (1)$$

where

$A = 249.4$ (S.E. = 74.6)
$B = 367.9$ (S.E. = 148.3)
S.E. estimate = 6.2
No. of specimens = 17.

This regression line is shown in Fig. 6 and illustrates that the loss of strength which is coincidental with Haversian remodeling cannot be fully explained by a decrease in bone density. It appears that bone remodeling leads to a reduction in ultimate strength not only by causing a decrease in density, but also by creating an inherently weaker structure.

The results of the fatigue tests to failure are summarized in Fig. 7, which shows the relationships between cycles to failure (N), microstructure, and density. Primary bone specimens were significantly more fatigue-resistant than either secondary Haversian specimens or specimens having a mixed microstructure. The mean log of the cycles to failure for the 17 primary specimens was 4.911 (S.D. = 0.289). This corresponds to a mean fatigue life of 81,554 cycles for the primary bone specimens.

A linear regression analysis of the primary specimens revealed a weak but significant correlation between log N and density ($r^2 = 0.506$, $P > 0.01$). The relationship between the predicted cycles to failure ($\bar{N}$) and bone density (ρ, g/cm^3) was expressed as

$$\log \bar{N} = C\rho + D \text{ (Primary bone)} \qquad (2)$$

where

$C = 5.08$ (S.E. = 1.29)
$D = -5.10$ (S.E. = 2.55)
S.E. estimate = 0.209
No. of specimens = 17.

This regression line is shown in Fig. 7 and illustrates that the decrease in fatigue life which is coincidental with Haversian remodeling cannot be fully explained by a decrease in bone density. Similar results were obtained from an earlier study (Carter *et al.*, 1976).

The results of the residual strength test are shown in Fig. 8, in which tensile strength is plotted against fatigue cycles. The results of the tensile tests without fatigue loading are also shown. As anticipated, the data of Fig. 8 exhibit a great deal of scatter. To extract meaningful information from these data, the effects of microstructure and density were considered.

Most of the specimens consisted entirely of primary bone containing woven-fibered bone and irregular primary osteons. Some specimens contained both primary bone and secondary Haversian bone. A few specimens had a secondary Haversian microstructure consisting entirely of secondary osteons and interstitial bone. Using cross section photomicrographs,

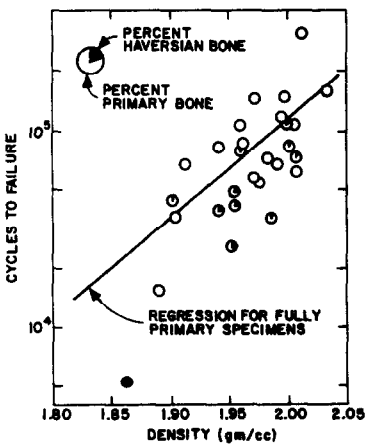

Fig. 7. Cycles to failure vs density for fatigue specimens.

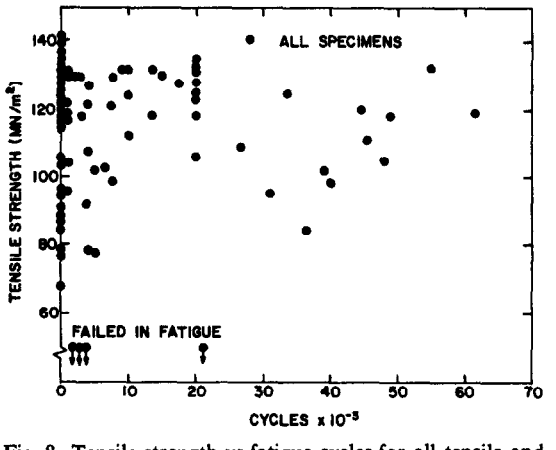

Fig. 8. Tensile strength vs fatigue cycles for all tensile and residual strength specimens.

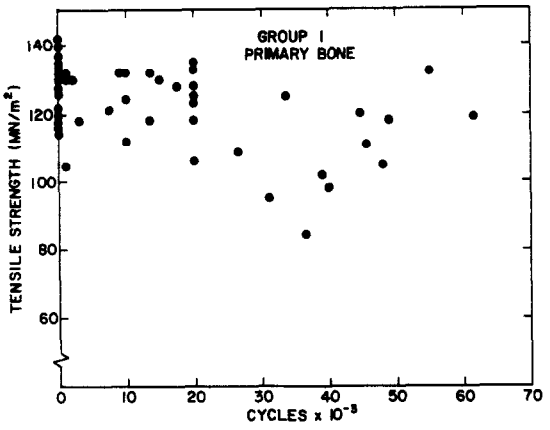

Fig. 9. Tensile strength vs fatigue cycles for specimens of microstructure Group (1)(primary structure).

the specimens were separated into four microstructure groups (see Carter *et al.*, 1976):

Group (1).
Fully primary bone structure.
Group (2).
Primary bone structure with indications of initial Haversian remodeling (less than 5% secondary Haversian bone).
Group (3).
Evidence of significant Haversian remodeling (greater than 5% secondary Haversian bone with the average specimen being approx. 40% secondary Haversian bone).
Group (4).
Fully secondary Haversian bone structure.

The data of Fig. 8 were then replotted on four separate graphs (Figs. 9, 10A–C) corresponding to the microstructure groups listed above. Since most of the specimens had a primary structure, only Fig. 9 (corresponding to Group (1)) presented enough data to allow meaningful conclusions to be drawn about residual strength during fatigue. The average life of the primary fatigue specimens was 81,554 cycles (mean log 4.911, S.D. 0.289) and the ultimate strength of the primary specimens that were not fatigued was 127.8 MN/m^2 (S.E. 1.9). The 29 primary residual strength specimens were fatigued to an average of 25,586 cycles (S.D. 16,501) and had a mean residual strength of 117.5 MN/m^2 (S.E. 2.4). The loss of tensile strength exhibited by the residual strength specimens was statistically significant ($P < 0.01$) and suggests that specimens fatigued to 31% of their fatigue lives showed approximately an 8% loss of tensile strength.

Residual strength data are often shown as a plot of residual strength ratio ($\sigma/\bar{\sigma}_0$) against fatigue life ratio ($n/\bar{N}$). Since density measurements were made for each specimen, it was possible to predict an initial ultimate strength ($\bar{\sigma}_0$) and a fatigue life ($\bar{N}$) for each primary bone specimen based on equations (1) and (2) respectively. On the basis of these predictions, the data of Fig. 9 were adjusted for bone density and the residual strength ratio and fatigue life ratio were estimated. These calculations were made using the following equations:

$$\left(\frac{\sigma}{\bar{\sigma}_0}\right)_i = \frac{\sigma_i}{249.4\rho_i - 367.9} \tag{3}$$

$$\text{S.E. estimate} \simeq 0.05\left(\frac{\sigma}{\bar{\sigma}_0}\right)_i.$$

$$\left(\frac{n}{\bar{N}}\right)_i = \frac{n_i}{5.08\rho_i - 5.10} \tag{4}$$

$$\text{S.E. estimate} \simeq 0.5\left(\frac{n}{\bar{N}}\right)_i,$$

where

σ = tensile strength
n = no. of fatigue cycles
$\bar{\sigma}_0$ = predicted initial tensile strength
$\bar{N}$ = predicted cycles to failure
ρ = specimen density
i = subscript denoting ith specimen ($i = 1, 2, 3, \ldots, 46$ for tensile specimens and residual strength specimens).

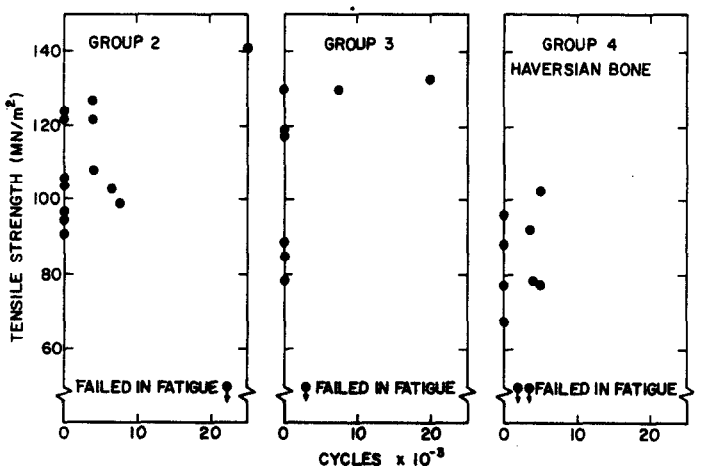

Fig. 10(A), (B), (C). Tensile strength vs fatigue cycles for specimens of microstructure Group (2), Group (3), Group (4).

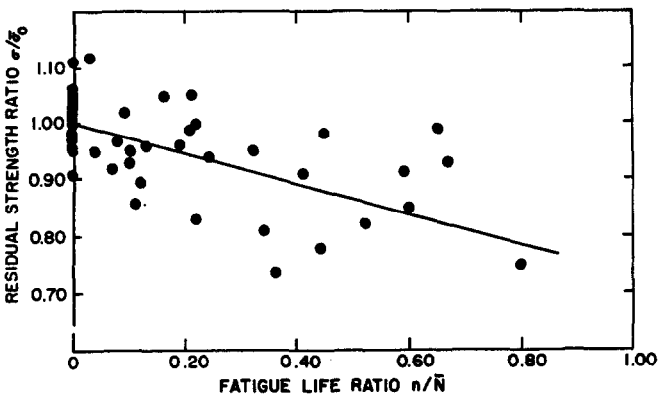

Fig. 11. Residual strength ratio vs fatigue life ratio for primary bone specimens.

The results of these calculations are shown in Fig. 11. The basic relation between strength and fatigue cycles is similar to that shown in Fig. 9. The data scatter, however, has been reduced.

Notice that equation (3) provides a much better estimate of residual strength ratio than equation (4) does for fatigue life ratio (based on S.E. of estimates). For example, consider a specimen with a predicted residual strength ratio of 0.80 and a predicted fatigue life ratio of 0.50. The standard errors of these estimates suggest that the *true* residual strength ratio is between 0.76 and 0.84 and the *true* fatigue life ratio is between 0.25 and 0.75 (confidence level 67%). The poorer prediction for fatigue life ratio is due to the data scatter observed in fatigue testing. The fact that the standard error of the estimate of $(n/\bar{N})$ increases linearly with $(n/\bar{N})$ explains the increased data scatter of Fig. 11 at higher fatigue life ratios.

Residual stiffness

Specimens with a homogeneous microstructure subjected to tensile fatigue tests of less than 1,000 cycles exhibited a gradual and progressive loss of stiffness throughout the testing period. This loss of stiffness was accompanied by an increasingly nonlinear loading behavior and a progressive increase in hysteresis. Figure 12 shows stress/strain curves at selected loading cycles (n) for a typical specimen. Failure of this specimen occurred at 401 cycles ($N = 401$). In Fig. 13 the ratio of the secant modulus of elasticity (E) to the initial secant modulus (E_0) is plotted as a function of fatigue life ratio $(n/\bar{N})$ for the same specimen. At failure, specimen stiffness had decreased by over 20%.

Specimens which had an inhomogeneous microstructure did not exhibit as great a loss in stiffness as shown in Fig. 13. In these specimens most of the damage was localized to a weak region in the gage length which was usually a small area of secondary Haversian bone. Since the extensometer knife edges were 25.4 mm apart, the apparent loss of stiffness over the total gage length was smaller than that at the site of the most severe damage.

Fracture surfaces

Specimens subjected to rotating bending fatigue tests to failure presented fracture surfaces which were dependent upon specimen microstructure and fatigue life. The fracture surfaces of fully Haversian specimens were of two types: (1) a cup–cone type of surface (Fig. 14A) and (2) an oblique surface (similar to those observed by Sweeney *et al.* (1965) in compression tests of compact bone). In both cases it appears that frac-

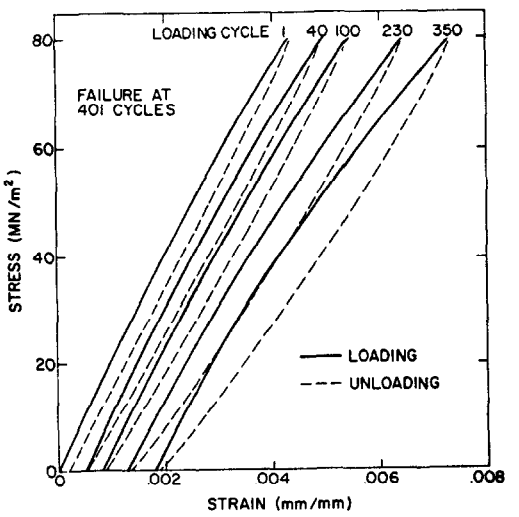

Fig. 12. Stress/strain curves in zero to tension fatigue.

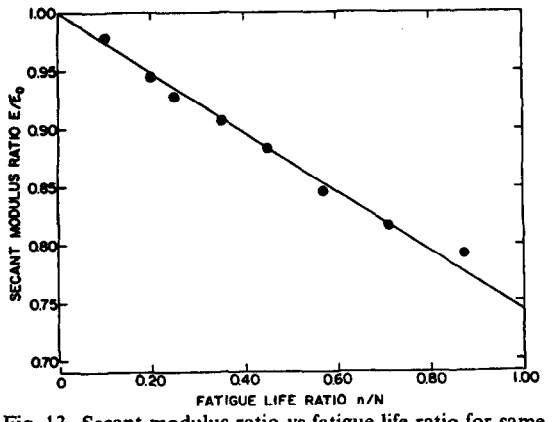

Fig. 13. Secant modulus ratio vs fatigue life ratio for same specimen shown in Fig. 12.

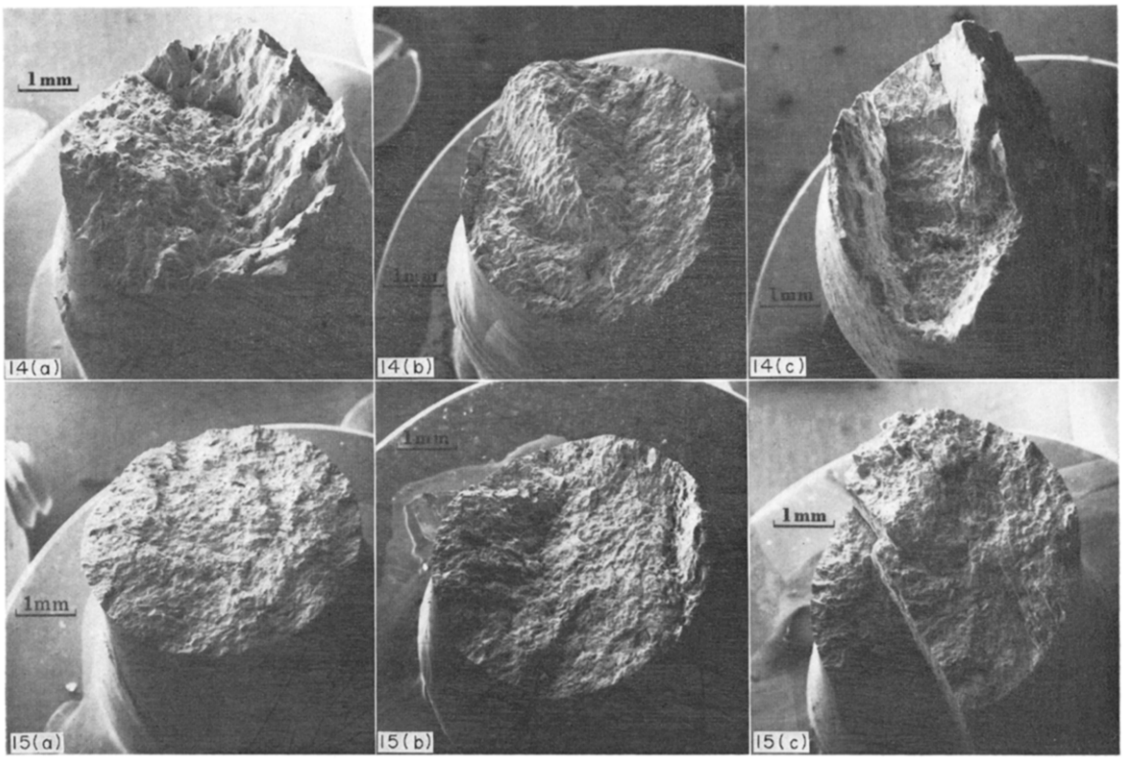

Fig. 14.(a) Rotating bending fatigue fracture surface of secondary Haversian specimen. A cup–cone type of surface is shown. (b) Rotating bending fatigue fracture surface of primary bone specimen. Oblique fracture planes are evident. (c) Rotating bending fatigue fracture surface of primary bone specimen. Oblique cracking and longitudinal splitting are seen.

Fig. 15.(a) Tensile fracture surface of primary bone specimen with no prior fatigue history. (b) Fracture surface of primary bone residual strength specimen. Estimated strength loss of 15%. (c) Fracture surface of primary bone residual strength specimen. Estimated strength loss of 19%.

ture was caused by progressive growth of cracks along planes of high shear stress. The primary bone specimens presented fatigue fracture surfaces of two types: (1) predominantly transverse fracture with multiple oblique planes (Fig. 14B), and (2) oblique planes interrupted by longitudinal splitting (Fig. 14C). Specimens subjected to higher stress amplitudes (97–142 MN/m^2) had fracture surfaces primarily of the first type. In some of these specimens a cup–cone type of surface was seen. Specimens subjected to lower stress amplitudes (resulting in longer fatigue lives) tended to exhibit more longitudinal splitting and more jagged fracture surfaces.

Primary bone specimens subjected to tensile tests (with no previous fatigue loading) presented flat, featureless fracture surfaces approximately normal to the loading direction (Fig. 15A). Most of the residual strength specimens (rotating bending fatigue followed by tensile test to failure) presented fracture surfaces which could not be distinguished from those of the tensile specimens. However, some of the residual strength specimens which showed a significant loss of strength after fatigue loading presented markedly different fracture surfaces.

Figure 15(B) shows the fracture surface of a residual strength specimen which had an estimated 15% loss of tensile strength after fatigue loading. The cup–cone appearance of the fracture surface is distinctly different from that of tensile specimens without fatigue loading. The oblique shear lip around the circumference of the waisted section probably reflects damage caused during fatigue loading. The flat central area appears to have been formed by crack propagation under tensile loading.

Figure 15(C) shows the fracture surface of a residual strength specimen which had an estimated 19% loss of tensile strength after fatigue loading. The fracture surface is interrupted by longitudinal splitting of the specimen. This splitting is similar to that found in some of the specimens that were fatigued to failure and was not found in any of the tensile specimens without prior fatigue loading. It therefore seems likely that the fatigue damage preceded the tensile loading and contributed to the fracture surface morphology.

DISCUSSION

Tests of initial tensile strength and fatigue to failure

The primary and secondary Haversian bone specimens subjected to tensile tests to failure (no prior fatigue loading) had mean strengths of 127.8 MN/n^2 (S.D. = 7.8) and 80.3 MN/n^2 (S.D. = 16.8) respectively. These strength values are consistent with those found in the investigations of Currey (1975) and Wright and Hayes (1976b) at a comparable strain rate of 0.001 sec^{-1}. Currey found a primary bone mean tensile strength of 126 MN/m^2 and a secondary Haversian bone mean tensile strength of 84 MN/m^2. Wright and Hayes observed mean tensile strengths for primary and secondary Haversian bone of 114 and 56 MN/m^2 respectively.

The rotating bending fatigue tests to failure of the 17 primary bone specimens in this study were conducted at a nominal stress amplitude of 86 MN/m^2 and a temperature of 37°C. The results of the fatigue study of Carter *et al.* (1976) suggest that the fatigue lives of these specimens can be estimated as:

$$\log 2\bar{N} = -7.79 \log (86) - 0.0206 (37) + 2.36\rho + 16.23$$
$$\log \bar{N} = 2.36\rho + 0.098 \quad (5)$$
$$\text{S.E. estimate} = 0.301.$$

The regression relationship between cycles to failure and density that was actually found for the 17 primary bone specimens reported in this article is:

$$\log \bar{N} = 5.08\rho - 5.10 \quad (6)$$
$$\text{S.E. estimate} = 0.209.$$

Figure 16 is a plot of the number of cycles to failure vs density for the 17 primary bone specimens. Also shown are the linear regression of these test data (equation 2) and the regression that would be predicted by equation (5). The fatigue to failure data of the present study suggest that density may have a stronger influence on fatigue life than was found by Carter *et al.* (1976). However, the predictions of fatigue life based on the analysis presented in the previous study are not unreasonable since most of the data points of this study fall within the scatter band of the earlier prediction.

Compact bone fatigue behavior

The results of this study indicate that repeated loading of bone causes immediate and progressive loss of both ultimate strength (Fig. 11) and stiffness (Fig. 13). In addition, a marked increase in nonlinearity and hysteresis of the stress/strain curves was observed during repeated loading. Similar fatigue behavior observed in concrete and composite materials is attributed to cumulative microcracking, debonding, void growth, and fiber breakage (Salkind, 1972; Neville, 1972). The fatigue characteristics of compact

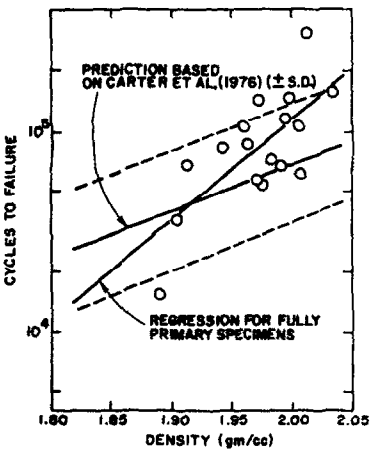

Fig. 16. Comparison of primary bone fatigue tests with predictions based on Carter *et al.* (1976).

bone are distinctly different from those of metals, which do not exhibit a loss of stiffness or ultimate strength until a fatigue crack is initiated by damage due to plastic flow (Yang and Trapp, 1974; Salkind, 1972). These findings strongly suggest that the post-yield regime of compact bone is not evidence of true plasticity (as suggested by Burstein *et al.*, 1973), but the result of diffuse structural damage.

Compact bone in compression is stronger and exhibits a smaller postyield regime than in tension (Reilly and Burstein, 1974; Burstein *et al.*, 1973). This behavior in monotonic loading is similar to that of glass-fiber reinforced cement (GRC), a composite of two brittle materials (Allen, 1971). Fatigue tests of GRC in tension cause a reduction in modulus which is strikingly similar to that seen with the bone specimens of this investigation. Allen (1971) noted that the GRC modulus reduction in fatigue is caused by cement cracking. Although there can be no direct physical analogy drawn between bone and GRC, the comparison of mechanical properties illustrates that one need not rely on the concepts of plastic flow or crazing to explain the nonelastic behavior of bone. Microscopic examination of bone specimens after repeated loading showed that debonding and microcracking are major damage modes (Carter and Hayes, 1977).

SUMMARY

An investigation of the loss of strength and stiffness of compact bone during fatigue was conducted. To study the effect of repeated loading on bone strength, primary bone specimens were machined from bovine femora. The mean ultimate strength of 17 specimens was determined from longitudinal tensile tests to be 127.8 ± 1.9 (S.E.) MN/m^2. Twenty-nine specimens were subjected to rotating bending fatigue loading which averaged 31% of the expected fatigue life and then loaded to failure in tension to determine their residual strengths. The mean residual strength was 117.5 ± 2.4 (S.E.) MN/m^2. This strength reduction caused by fatigue was significant at the $P < 0.01$ level and is comparable to the strength reductions seen in fatigue of composite materials. To examine the loss of stiffness during fatigue, longitudinally oriented specimens were subjected to cyclic tensile tests at a loading frequency of 0.1 Hz. An extensometer was used to record stress/strain curves which showed a progressive loss of specimen stiffness accompanied by an increasingly nonlinear loading behavior and hysteresis during fatigue.

These studies show that repeated loading of bone can cause a progressive loss of stiffness and ultimate strength. A similar fatigue behavior is seen in composite materials and is attributed to cumulative microcracking, debonding, void growth, and fiber breakage. These fatigue characteristics are distinctly different from those of metals, which do not exhibit a loss of stiffness or strength until a fatigue crack is initiated by damage due to plastic flow. These results further suggest that bone yielding observed in monotonic loading to failure is caused by diffuse structural damage such as microcracking and debonding.

Acknowledgements—The authors thank Arthur Leach for assisting in specimen preparation and Loren Anderson for the SEM photomicrographs.

REFERENCES

Allen, H. G. (1971) Stiffness and strength of two glass-fibre reinforced cement laminates. *J. Comp. Mat.* **5**, 194–207.

Ascenzi, A. and E. Bonucci (1976) Mechanical similarities between alternate osteons and cross-ply laminates. *J. Biomechanics* **9**, 65–71.

Burstein, A. H., J. D. Currey, V. H. Frankel and D. T. Reilly (1972) The ultimate properties of bone tissue: the effects of yielding. *J. Biomechanics* **5**, 34–44.

Burstein, A. H., D. T. Reilly and V. H. Frankel (1973) Failure characteristics of bone and bone tissue. *Perspectives in Biomedical Engineering* (Edited by R. M. Kenedi) Univ. Park Press, London.

Burstein, A. H., J. J. M. Zika, K. G. Heiple and L. Klein (1975) Contribution of collagen and mineral to the elastic-plastic properties of bone. *J. Bone Jnt Surg.* **57A**, 956–961.

Carter, D. R. (1976) *The Fatigue Behavior of Compact Bone*, Ph.D. dissertation, Stanford University.

Carter, D. R. and W. C. Hayes (1976) Fatigue life of compact bone—I. Effects of stress amplitude, temperature and density. *J. Biomechanics* **9**, 27–34.

Carter, D. R. and W. C. Hayes. Compact bone fatigue damage—II. A microscopic examination. *Clin. Orthop.*, (to be published).

Carter, D. R., W. C. Hayes and D. J. Schurman (1976) Fatigue life of compact bone—II. Effects of microstructure and density. *J. Biomechanics* **9**, 211–218.

Chamay, A. (1970) Mechanical and morphological aspects of experimental overload and fatigue in bone. *J. Biomechanics* **3**, 263–270.

Chamay, A. and P. Tschantz (1972) Mechanical influences in bone remodeling. Experimental research on Wolff's law. *J. Biomechanics* **5**, 173–180.

Currey, J. D. (1975) The effects of strain rate, reconstruction, and mineral content on some mechanical properties of bovine bone. *J. Biomechanics* **8**, 81–86.

Devas, M. B. (1965) Stress fractures of the femoral neck. *J. Bone Jnt Surg.* **47B**, 728–737.

Devas, M. (1975) *Stress Fractures.* Churchill Livingstone, London and New York.

Evans, F. G. (1973) *Mechanical Properties of Bone.* Charles C. Thomas, Springfield, Ill.

Forrest, P. G. (1962) *Fatigue of Metals.* Addison-Wesley, Reading, Mass.

Frost, H. L. (1966) *Bone Dynamics in Osteoporosis and Osteomalacia.* Charles C Thomas, Springfield, Ill.

Gray, R. J. and G. K. Korbacher (1974) Compressive fatigue behavior of bovine compact bone. *J. Biomechanics* **7**, 287–292.

Morris, J. M. and L. D. Blickenstaff (1967) *Fatigue Fractures.* Charles C Thomas, Springfield, Ill.

Nash, C. D. (1966) Fatigue of self-healing structures: A generalized theory of fatigue failure. Amer. Soc. of Mech. Eng. Publ. No. 66-WA/BHF-3, New York.

Neville, A. M. (1972) *Properties of Concrete.* Pitman Publ., New York.

Owen, M. J. and R. J. Howe (1972) The accumulation of damage in a glass-reinforced plastic under tensile and fatigue loading. *J. Phys. D.: Appl. Phys.* **5**, 1637–1649.

Radin, E. L., H. G. Parker, J. W. Pugh, R. S. Steinberg, I. L. Paul and R. M. Rose (1973) Response of joints

to impact loading—III. Relationship between trabecular microfractures and cartilage degeneration. *J. Biomechanics* **6**, 51–57.

Reed-Hill, R. E. (1964) *Physical Metallurgy Principles*. D. Van Nostrand, Princeton, N.J.

Reilly, D. T. and A. H. Burstein (1974) The mechanical properties of cortical bone. *J. Bone Jnt Surg.* **56-A**, 1001–1022.

Salkind, M. J. (1972) *Composite Materials: Testing and Design*. Amer. Soc. for Testing and Materials Publ. No. 497, 143, ASTM, Philadelphia.

Schneider, R. and J. J. Kaye (1975) Insufficiency and stress fractures of the long bones occurring in patients with rheumatoid arthritis. *Radiol.* **116**, 595–599.

Sedlin, E. D. and C. Hirsch (1966) Factors affecting the determination of physical properties of femoral cortical bone. *Acta orthop. scand.* **37**, 29–48.

Sweeney, A. W., R. K. Byers and R. P. Kroon (1965) Mechanical characteristics of bone and its constituents. *Amer. Soc. Mech. Eng. Publ.* No. 65-WA/HUF-7, New York.

Wall, J. C., S. Chatterji and J. W. Jeffrey (1970) On origin of scatter in results of human bone strength tests. *Med. Biol Engng* **8**, 171–180.

Wright, T. M. and W. C. Hayes (1976a) The fracture mechanics of fatigue crack propagation in compact bone. *J. Biomed. Mater. Res. Symp.* **7**, 637–648.

Wright, T. M. and W. C. Hayes (1976b) Tensile testing of bone over a wide range of strain rates: Effects of strain rate, microstructure and density. *Med. Biol. Engng.* **14**, 671–680.

Yang, J. N. and W. J. Trapp (1974) Reliability analysis of aircraft structures under random loading and periodic inspection. *AIAA J.* **12**, 1623.

NOMENCLATURE

σ	tensile strength
$\bar{\sigma}_0$	predicted initial tensile strength (MN/m^2)
ρ	dry bone density (g/cm^3)
A, B	regression constants of equation (1)
n	fatigue cycles (cycles)
N	fatigue cycles to failure (cycles)
$\bar{N}$	predicted fatigue cycles to failure (cycles)
C, D	regression constants of equation (2)
i	subscript denoting i^{th} specimen
E_0	secant modulus of elasticity of first loading cycle (MN/m^2)
E	secant modulus of elasticity (MN/m^2).